Wangbi Tablet Regulates the Osteogenic Homeostasis by MiR335-5p through the Wnt/β-catenin Signaling Pathway and the RANK/RANKL/OPG System: An in Vivo Animal Study

Xinyan Zhang
Beijing University of Chinese Medicine
Longji Sun
Beijing University of Chinese Medicine
Huilan Zheng
Beijing University of Chinese Medicine
Qingwen Tao
Department of TCM Rheumatology China-Japan Friendship Hospital
Zeran Yan
Department of TCM Rheumatology China-Japan Friendship Hospital
Tongliang Zhou
Institute of Clinical Medicine, China-Japan Friendship Hospital
Hong Li
Institute of Clinical Medicine, China-Japan Friendship Hospital
Yuting Bian
Beijing University of Chinese Medicine
Chang Gan
Beijing University of Chinese Medicine
Jianming Wang (doctorwangjm@sina.com)
Department of TCM Rheumatology China-Japan Friendship Hospital

Research Article

Keywords: Rheumatoid Arthritis, Bone Destruction, Osteoblast Homeostasis, MiR335-5p, Traditional Chinese Medicine

Posted Date: September 27th, 2022

DOI: https://doi.org/10.21203/rs.3.rs-2081455/v1

Abstract

OBJECTIVE: This study investigated how the classic Chinese patent drug Wangbi tablet (WBT) for treating rheumatoid arthritis (RA) regulates the osteogenic homeostasis through miR335-5p through the Wnt/β-catenin pathway and the RANK/RANKL/OPG system.

METHODS: The kidney deficiency pattern modeling rats were established by using castration operation. Collagen-induced arthritis (CIA) was performed on rats for joint modeling. WBT and methotrexate (MTX) gavage interventions were used according to the group situation and body weight. The ankles of the rats were reconstructed in three dimensions using micro-computed tomography (micro-CT). The relative expressions of Wnt3a, Wnt10b, β-catenin, DKK1, RUNX2, DICER1, TRAP6 and NFATC1 in rat ankle bone tissues were measured using Western-Blot (WB).

RESULTS: In this study, we found that WBT promoted the expression of Wnt3a, Wnt10b, β-catenin and miR335-5p, decreased the expression of DKK1, promoted the Wnt/β-catenin signalling pathway, increased the expression of osteogenic markers Runx2 and DICER1, and also regulated the RANKL/OPG balance in the affected joint bone tissue. The expression of osteogenic markers TRAP6 and NFATC1 was decreased, and the bone destruction of rats in CIA group and kidney deficiency pattern CIA group was improved.

Conclusion: WBT can promote the expression of miR335-5p, inhibit the expression of DKK1, regulate the Wnt/β-catenin signaling pathway and the RANK/RANKL/OPG system in the ankle bone tissue of CIA and kidney deficiency pattern CIA rats, and regulate the balance of osteoclasts to treat bone destruction in RA.

Research Background

Rheumatoid arthritis (RA) is a chronic, systemic autoimmune disease with a high morbidity and disability rate, with synovitis and vasculitis as the main pathological features. Bone destruction is one of the typical pathological features of RA patients, with more than 10% of RA patients presenting with bone destruction 8 weeks after onset [1–2]. Excessive bone resorption by local osteoclasts (OC) and insufficient bone formation by osteoblasts (OB) are important causes of imbalance in bone homeostasis [3].

OC plays a key role in bone destruction in RA. OC are mononuclear macrophages that are differentiated from myeloid progenitor cells in the bone marrow and stimulated by various chemokines, transcription factors, cytokines, and other signaling factors to fuse into multinucleated cells and eventually activate into a multinucleated giant cell with bone resorption function [4]. The process of OC differentiation is modulated by a variety of signaling molecules, RANKL is the most critical factor throughout the process [5]. In recent years, more and more studies have suggested that RANKL is an important target for the treatment of bone destruction in RA. It has been shown that RANKL is highly expressed in the affected joints of collagen-induced arthritis (CIA) mice and inhibition of RANKL expression can inhibit OC formation and alleviate joint inflammation and bone destruction in CIA mice [6–8].

OB plays an important role in the maintenance of bone homeostasis. OB is mainly differentiated from mesenchymal progenitor cells in the stroma of the inner and outer periosteum and bone marrow, and can specifically secrete a variety of bioactive substances that regulate bone formation and reconstruction processes [9]. The Wnt/β-catenin pathway is one of the important signaling pathways in the differentiation of OB and the regulation of bone formation, bone homeostasis and bone density. wnt3a, wnt4b, wnt10 and wnt16 are important for maintaining osteoblast homeostasis [10–11]. Recent studies [12–13] have suggested that DKK1 is a key target for the regulation of bone homeostasis through the Wnt/β-catenin pathway, and that the proliferation and differentiation of osteoblasts can be regulated by inhibiting DKK1 expression and activating the Wnt/β-catenin pathway.

miR335-5p, located at 7q32.2, regulates the cytoskeleton .etc and is closely associated with markers of bone metabolism. Previous studies have shown[14] that miR335-5p is an important regulator of osteogenic differentiation and plays a key role in maintaining the osteogenic capacity of bone-forming cells. Another study showed[15–16] that miR335-5p could enhance OB proliferation and differentiation by downregulating DKK-1 expression and activating the Wnt/β-catenin pathway; meanwhile, in OC, miR-355-5p downregulated RANKL expression and inhibited OC proliferation. Previous studies have suggested that extracts of different Chinese medicines can effectively treat bone destruction in RA from multiple targets and pathways, but the exact molecular mechanisms are not clear [17].

In this study, we investigated the mechanism by which WBT, a classical Chinese medicine for the treatment of RA, regulates osteogenic homeostasis through miR335-5p regulating the Wnt/β-catenin pathway and the RANK/RANKL/OPG pathway.

Materials And Methods

Animals

SD rats of SPF grade, 96 rats, male and female, 6 weeks old, body mass (200±20) g, purchased from Beijing HFK Bio-Technology Company. The experiments were reviewed and approved by the Experimental Animal Welfare Ethics Committee of the China-Japan Friendship Hospital, approval number: zryhyy21-21-03-03.

Drug

WBT tablets, specification: 0.5g/tablet, GMP Z20044066, manufactured by Liaoning Good Nurse Pharmaceutical (Group) Co Ltd; Methotrexate tablets, specification: 2.5mg/tablet, GMP H31020644, manufactured by Shanghai Xinyi Pharmaceutical Factory.

Main Reagents

Immunization Grade Bovine Type II Collagen (Item No. 20022), Freund's Incomplete Adjuvant (Item No. 7002), Chondrex; Protein Extract (Item No. MDL91201), Protease Inhibitor (Item No. MD912893), BCA

Protein Concentration Assay Kit (Item No. MD913053), SDS-PAGE Prepared Gel Kit (Item: MD911919), DEPC (Item: MD911875), Interleukin 4 (IL-4) Kit (Item: MD123461), IL-1β Kit (Item: MD6758), OPG Kit (Item: MD123455), RANKL kit (item no. MD120008), MDL; medium protein molecular weight marker (item no. 26617), Thermo; β-actin (item no. ab8226), abcam; NFATc1 (item no. A1539), TRAF6 (item no. A16991) DKK1 (item no. A2562), WNT3A (Item: A0642), WNT10B (Item: A16717), β-catenin (Item: A19657), abclonal; TRIZOL (Item: 10296028), Invitrogen; anhydrous ethanol (Item: 10009218), isopropanol (Item: 40064360), abcam; NFATc1 (Item: A1539), TRAF6 (Item: A16991) DKK1 (Item. (item no. 40064360), Sinopharm; UltraPure Agarose (item no. 16500100), SuperScript III RT reverses transcription kit (item no. 11752050), Sybr qPCR mix (item no. 4472920), ABI-Invitrogen.

Main instruments

Microscope (DM3000 model), Leica; Decolorisation shaker (TS-100 model), Haimen Kylin-Bell Lab Instruments Company; Electrophoresis apparatus (BG-subMIDI model), Beijing Baygene Biotech Company; Cryogenic centrifuge (3-30K model), Sigma, Germany; SDS-PAGE electrophoresis system (Mini-PROTEAN® Tetra Cell with Mini Trans-Blot® Module And PowerPac™ Universal Power Supply), Enzyme Labeler (Model 550), BIO-Rad, USA; Gel Imaging System (GelDoc-It310), UVP, USA; Chemiluminescence Imaging System (ChemiScope 6100), CLINX, China; benchtop high-speed frozen centrifuge (LEGEND MICRO 21R), spectrophotometer (Nanodrop lite), THERMO; electrophoresis instrument (EPS 300), gel imager (2500), biorad; fluorescence quantitative PCR instrument (StepOne Software), Applied biosystems (USA), micro-CT (Siemens INVEON mmCT).

Animal grouping and models preparation

After 1 week of acclimatization, the rats were grouped by the random number table method with 12 animals in each group. They were divided into 8 groups: blank control group, CIA group, renal deficiency group, kidney deficiency pattern CIA group, CIA + WBT group, kidney deficiency pattern + WBT group, kidney deficiency pattern CIA + WBT group, and CIA + MTX group. The kidney deficiency pattern model was firstly prepared using the castration operation (removal of both ovaries and testes), and then the collagen-induced arthritis (CIA) model was prepared 4 weeks later using bovine type II collagen and incomplete Freund's adjuvant induction.

Medications

The usual clinical dose of WBT is 2g tid, i.e. 6g/d. According to the "Human and Animal Body Surface Area Conversion Equivalent Dose Ratio Table", if the clinical dose for humans is Xmg/kg, the dose for rats = 6.3Xmg/kg, e.g. the human body weight is 60kg, the rat dose is 0.63g/kg QD; once a day for 8 weeks, dissolved in physiological saline to make a solution with a concentration of 0.25g/ml, ready to use. The usual clinical dose of methotrexate tablets is 10mg qw, and the calculated dose for rats is 1.05mg/kg qw; once a week for 8 weeks, dissolved in saline to make a solution of 0.25mg/ml, ready to use.

After the model was successfully replicated, the animals were performed intragastric administration. Apart from the methotrexate once a week in the CIA+MTX group, also saline the rest of the week. Equal amounts of saline every day in the blank control group, the CIA group, the kidney deficiency pattern group and the kidney deficiency pattern CIA group. The specific animal groups and intervention methods are shown in Table 1.

Table1

Sampling Method

In each group, blood was obtained by execution at the end of the intragastrical cycle. Whole blood was collected from the abdominal aorta and centrifuged at 3000r/min for 15 min (10 cm radius) to obtain the supernatant serum, which was stored at -80°C for subsequent enzyme-linked immunosorbent assay (Elisa). After execution, the hind limb ankle joints were quickly exposed and cut off bilaterally to remove excess skin and soft tissue around the joints. The left hind limb was fixed in 4% paraformaldehyde for 48h, then the residual fluid was washed off the joint with running water and the joint was placed in EDTA decalcifying solution, which was changed periodically until a 1ml syringe needle could easily penetrate into the joint bone as the criterion for complete decalcification, which took approximately 2 months to prepare for paraffin sectioning. The right hind limb was placed in a labeled specimen bag and immediately frozen at -80℃ for Real-Time quantitative fluorescence PCR (Real-Time PCR) and protein immunoblotting (Western Blot, WB).

Observations and methods

Elisa test for IL-1β, IL-4, OPG and RANKL in rat serum

The concentrations of IL-6, IL-1, TNF-α, IL-4, IL-10 and OPG in serum were measured according to the operation method of Elisa kit instructions. The absorbance (OD) was measured at 450nm. The regression equation of the standard curve was calculated according to the concentration and OD value, and the logistic curve (four parameters) was used to fit the model.

Real-Time PCR detection of mir-335-5p, RANKL and OPG expression in rat ankle bone tissue

Total RNA was extracted from the samples by Trizol method, and the concentration and purity of RNA were determined using a nucleic acid concentration meter. cDNA was synthesized by reverse transcription using an invitrogen reverse transcription kit, superscript III. A Real-time PCR reaction system was established and reacted on a fluorescent quantitative PCR instrument. β-actin was used as an internal reference. The relative expression of the genes was calculated by the $^{\triangle\triangle}$CT attenuation. The primer design of this experiment is shown in Table 2.

(Table 2)

Western blot detection of DKK-1, wnt3a, wnt10b, β-catenin and RANK expression in rat ankle bone tissues

Rat ankle tissues were homogenized with liquid nitrogen, lysed in an ice bath, centrifuged at 4℃ and 12000rpm for 15min, and the supernatant was collected. The protein concentration was determined by BCA protein quantification method. The protein bands separated on the gel were transferred to PVDF membrane by SDS-PAGE gel electrophoresis. This membrane was sealed and preserved in the blocking solution for 1h. The primary antibody was diluted in the blocking solution and reacted overnight at 4°C. The secondary antibody was diluted 300 times with 1×TBST and applied for 60 min. The bands were analysed for grey scale values and relative protein expression.

Detection of bone erosion in rat ankle joint by micro-CT

The ankles of rats were fixed in 4% paraformaldehyde for 48h and the residual fluid was washed off the joint with running water. A micro-CT scan was performed and the bone was reconstructed in three dimensions to assess the bone erosion.

Statistical methods

SPSS 25.0 statistical software was used for data analysis. The data results were presented in graphical form. Measurement data were described as mean ± standard deviation. As to the comparison among the groups, one-way ANOVA was used if the data were normally distributed and met the variance, and non-parametric tests were used if they did not follow a normal distribution or did not meet the variance. All statistical tests were two-sided, and differences were considered statistically significant at $p<0.05$.

Results

effects of WBT on micro-CT of rat foot and ankle

The articular cartilage surfaces were intact in the blank control group, the kidney deficiency pattern group, and the kidney deficiency pattern +WBT group; compared with the blank control group, the CIA group, the kidney deficiency pattern CIA group, the kidney deficiency pattern CIA+WBT group, the CIA+WBT group, and the CIA+MTX group all had different degrees of structural damage to the articular cartilage surfaces and narrowing or loss of joint space; compared with the CIA group, the CIA+MTX group had no significant changes to the articular cartilage surfaces, and the CIA+WBT group had partial damage to the articular cartilage surfaces and were relatively intact. The articular cartilage surface in the CIA+WBT group had partial destruction and was relatively intact; compared with the kidney deficiency pattern CIA group, the articular cartilage surface in the kidney deficiency pattern CIA+WBT group was relatively intact and the joint gap was clear (Figure 1).

(Figure 1)

Effect of WBT on miR335-5p

Compared with the blank control group, miR335-5p mRNA expression in the ankle bone tissue of rats in the kidney deficiency pattern CIA group was significantly decreased (P< 0.05). miR335-5p mRNA expression in the ankle bone tissue of rats in the kidney deficiency pattern CIA+WBT group was significantly increased (P< 0.01); compared with the kidney deficiency pattern CIA group, miR335-5p mRNA expression in the kidney deficiency pattern CIA+WBT group was significantly increased (P< 0.01) (Figure 2).

(Figure 2)

Effect of WBT on Wnt/β-catenin signaling pathway and osteogenesis-related markers

Compared with the blank control group, the relative expressions of Wnt3a, Wnt10b and β-catenin in the ankle bone tissue of the kidney deficiency pattern CIA group were significantly lower (P< 0.01) (Figure 3, a-c); the relative expressions of RUNX2 and DICER1 in the ankle bone tissue of the kidney deficiency pattern CIA group were significantly lower (P< 0.05) (Figure 3, e,f); The relative expression of RUNX2 was significantly lower (P< 0.05) in the ankle bone tissues of the kidney deficiency pattern group and the CIA group compared with the blank control group (Figure 3,e); the relative expression of DKK1 was significantly higher (P< 0.01) in the ankle bone tissues of the kidney deficiency pattern group and the CIA group compared with the blank control group (Figure 3,d).

Compared with the kidney deficiency pattern CIA group, the relative expression of Wnt3a, Wnt10b, β-catenin, and RUNX2 in the ankle bone tissue of the kidney deficiency pattern CIA+WBT group was significantly higher (P< 0.01) (Figure 3, a-c, e), the relative expression of DICER1 was significantly higher (P< 0.05) (Figure 3, f), and the relative expression of DKK1 was significantly lower (P< 0.01) (Figure 3, d).

Compared with the kidney deficiency pattern group, β-catenin and DICER1 were significantly higher in the kidney deficiency pattern + WBT group (P< 0.01, P< 0.05) (Figure 3, c, f). Compared with the CIA group, the relative expression of β-catenin and RUNX2 was significantly higher in the CIA+WBT group (P< 0.01) (as in Figure 3, c, e)

(Figure 3)

Effect of WBT on RANK/RANKL/OPG system and bone breaking related markers

Compared with the blank control group, the concentration of RANKL in serum was significantly higher (P< 0.05) and the concentration of OPG was significantly lower (P< 0.01) in the kidney deficiency pattern CIA group (Figure 4, a,b), while the ratio of RANKL/OPG was higher but not significantly different (P> 0.05) (Figure 4, c); compared with the blank control group, the concentration of RANKL in bone tissue was significantly higher in the kidney deficiency pattern CIA group (P< 0.05) (Figure 4, d), the concentration of OPG was significantly lower (P< 0.01) (Figure 4, e) and the ratio of RANKL/OPG was significantly higher (P< 0.01) in the bone tissue of the kidney deficiency pattern CIA group compared with the blank control group (Figure 4, f). There were no significant differences in RANKL, OPG and RANKL/OPG in serum in the kidney deficiency pattern CIA+WBT group compared with the kidney deficiency pattern CIA group (Figure

4, a-c); the concentration of RANKL in bone tissue was significantly higher (P<0.05) in the kidney deficiency pattern CIA+WBT group compared with the kidney deficiency pattern CIA group (Figure 4, d), and the concentration of OPG was significantly lower (P< 0.01) (Figure 4, e) and the ratio of RANKL/OPG was significantly higher (P< 0.01) (Figure 4, f).

(Table 3)

(Figure 4)

Compared with the blank control group, the relative expression of TRAP6 and NFATC1 in ankle bone tissue was significantly higher in the CIA and kidney deficiency pattern CIA groups (P< 0.01); compared with the kidney deficiency pattern CIA group, the relative expression of TRAP6 was significantly lower in the kidney deficiency pattern CIA +WBT group (P< 0.01) (Figure 5, a), and the relative expression of NFATC1 was significantly lower (P< 0.05) (Figure 5, b).

(Figure 5)

Effect of WBT on serum IL-1β and IL-4 in each group of rats

Compared with the blank control group, the serum concentrations of IL-1β were significantly higher (P<0.01) and IL-4 were significantly lower (P<0.01) in the CIA group and the kidney deficiency pattern CIA group (Figure 6, a, d), while the differences in serum IL-1β and IL-4 concentrations in the kidney deficiency pattern group were not significantly different (Figure 6, a, d). Compared with the CIA group, IL-1β concentrations in the CIA+WBT and CIA+MTX groups were significantly lower (P<0.01) (Figure 6, b), while serum IL-1β concentrations in the kidney deficiency pattern CIA group were significantly higher (P<0.01) (Figure 6, a). Compared with the kidney deficiency pattern CIA group, IL-1β concentration was significantly lower (P<0.01) and IL-4 concentration was significantly higher (P<0.01) in the kidney deficiency pattern CIA+WBT group (Figure 6, c, f).

(Figure 6)

Discussion

We detected Wnt/β-catenin signaling pathway-related proteins and osteogenic markers Runx2 and DICER1 by WB. In this study, we found that WBT could promote the expression of Wnt3a, Wnt10b and β-catenin, promote the expression of the Wnt/β-catenin signaling pathway, increase the osteogenic markers Runx2 and DICER1 expression and promote osteoblast proliferation and differentiation.

The Wnt/β-catenin signaling pathway is an important pathway for OB proliferation and differentiation. When Wnt protein binds to the Frizzled-LRP5/6 co-receptor complex, it increases the concentration of unphosphorylated β-catenin in the cytoplasm, which is then transferred to the nucleus to initiate the transcription of target genes, participating in the expression of several target genes, including BMP2 and Runx2, and regulating OB proliferation and differentiation. Its inhibitor DKK1 is closely related to

inflammatory bone loss and bone formation. DKK1 can inhibit OB cell proliferation and differentiation by targeting and blocking Wnt protein binding to the Frizzled-LRP5/6 co-receptor complex and decreasing the concentration of unphosphorylated β-catenin in the cytoplasm, thereby interfering with the Wnt/β-catenin signaling pathway. AT Shaw1 et al[19] showed that blocking DKK1 expression in an AIA mouse model significantly promoted new bone formation. In contrast, new bone formation was significantly less in AIA model mice in the presence of increased DKK1 expression. CenLuo et al [20] showed that excess iron death may inhibit osteoblast differentiation and cause bone loss by interfering with the classical Wnt/β-catenin signaling pathway. Divya Rai et al [21] showed that BMP2 pro-secretin can inhibit bone loss by increasing WntT3A, SOST, GSK3-β, and β-catenin expression, promoting Wnt/β-catenin signaling pathway expression and inhibiting hormone-induced bone loss.

We measured the levels of RANKL and OPG in serum and ankle bone tissues by Elisa and qt-PCR, respectively, and the expression of bone breaking markers TRAP6 and NFATC1 in ankle bone tissues by WB. In this study, we found that WBT regulated the balance of RANKL/OPG in the bone tissue of the affected joints, decreased the expression of the osteoclastic markers TRAP6 and NFATC1, and inhibited OC proliferation, differentiation and activity.

OC plays a key role in bone destruction in RA and its differentiation and maturation are regulated by the RANK/RANKL/OPG signaling pathway. The RANK receptors on the membrane surface of OC and its precursor cells bind specifically to RANKL to promote the differentiation and maturation of OC precursors and the activation of OC [22]. OPG is a RANKL decoy receptor, mainly produced by osteoblasts The RANKL/OPG ratio, known as a regulator of osteoclastogenesis, is an important determinant of bone resorption. Both upregulation of RANKL and downregulation of OPG can lead to bone loss [24]. Previous studies have shown that high expression of RANKL can be detected in the serum of RA patients, which may contribute to OC differentiation and lead to the development of bone destruction in RA [25]. Yuanyuan Ling et al[26] showed that Zhijing powder could inhibit osteoclastogenesis and improve arthritic bone erosion in CIA mice by regulating RANKL expression. Agnieszka Jura-Półtorak et al[27] showed that TNF inhibitors down-regulated the RANKL/OPG ratio in the serum of RA patients and inhibited bone destruction.

We found that WBT promoted miR335-5p expression in rat ankle bone tissue by detecting miR335-5p expression in all groups of rats. Previous studies have shown[15] that miR335-5p can activate the Wnt/β-catenin pathway and enhance osteoblast proliferation and differentiation by targeting the inhibition of DKK-1 expression. Gong M et al [28] found that miR-355-5p deletion could lead to high RANKL expression, which may result in OC over differentiation and osteolytic lesions. Collectively, WBT can promote miR335-5p expression and inhibit DKK1 expression, while regulating the Wnt/β-catenin signaling pathway and the RANK/RANK/OPG system.

We measured the serum levels of IL-1β and IL-4 by Elisa and found that WBT could increase the serum concentration of IL-4 and decrease the serum concentration of IL-1β. RA as a chronic autoimmune

disease, the imbalanced secretion of various cytokines plays a key role in RA bone destruction, including common pro-inflammatory factors such as IL-6, IL-17, IL-1, TNF-α, and common anti-inflammatory factors such as IL10, IL-4 and IFN-γ, and others, which have regulatory effects on T cells, B cells, synovial fibroblasts, OB and OC [29]. Previous studies have shown that IL-4 and IL-10 can inhibit the transcriptional expression of NFATc1 and suppress the secretion of pro-inflammatory factors such as TNF-α, IL-1 and IL-6.

Conclusion

WBT can promote the expression of miR335-5p, inhibit DKK1 expression, regulate the Wnt/β-catenin signaling pathway and RANK/RANKL/OPG system in the ankle bone tissue of CIA model and kidney deficiency pattern CIA model rats, and regulate the balance of OC and OB to treat RA bone destruction (Fig. 7).

(Fig. 7)

Abbreviations

CIA: collagen-induced arthritis; DICER1: Recombinant DICER Enzyme 1; DKK1: Dickkopf-related protein 1;IL: Interleukin; micro-CT: micro computed tomography; MTX: methotrexate;NFATC1: Recombinant Nuclear Factor Of Activated T-Cells, Cytoplasmic 1;OB: osteoblast; OC: Osteoclast; OPG: osteoclastogenesis inhibitory factor; PCR: Polymerase chain reaction; RANK: receptor activator of NF-KB ; RANKL: receptor activator of NF-KB ligand ; RUNX2: Runt-related transcription factor 2; RA: rheumatoid arthritis; TRAP6: PAR-1 agonist peptide; WBT: Wangbi Tablet;

Declarations

Authors' contributions:

XZ, LS, HZ and JW designed the study. XZ, LS and HZ collected and analyzed the data. XZ, LS, HZ, ZY and GC interpreted the data. XY, LS, YB wrote the first draft of the manuscript. JW, QT, TZ and HL revised the draft for the scientific content. The authors approved the final version of the manuscript.

Authors’ information

XZ, LS and HZ contributed equally to this work.

Source of funding: National Natural Science Foundation of China (82074223)

Availability of data and materials: The datasets used and/or analyzed during this study are available from the corresponding authors upon reasonable request.

Ethics approval and consent to participate:

The experiments were reviewed and approved by the Experimental Animal Welfare Ethics Committee of the China-Japan Friendship Hospital, approval number (approval number: zryhyy21-21-03-03) and adheres to the guidelines of Animal Research: Reporting of In Vivo Experiments.

Conflict of interest:

All authors declare no conflict of interest

Consent to publication:

all authors consent to the publication

Author details

1. Beijing University of Chinese Medicine, Beijing, 10029, Republic of China

2. Department of TCM Rheumatology China-Japan Friendship Hospital, Beijing, 10029, Republic of China

3. Institute of Clinical Medicine, China-Japan Friendship Hospital, Beijing, 10029, Republic of China

References

1. Schett G. Autoimmunity as a trigger for structural bone damage in rheumatoid arthritis. Mod Rheumatol. 2017 Mar;27(2):193–197. doi: 10.1080/14397595.2016.1265907. Epub 2017 Jan 9.
2. Panagopoulos PK, Lambrou GI. Bone erosions in rheumatoid arthritis: recent developments in pathogenesis and therapeutic implications. J Musculoskelet Neuronal Interact. 2018 Sep 1;18(3):304–319.
3. Tateiwa D, Yoshikawa H, Kaito T. Cartilage and Bone Destruction in Arthritis: Pathogenesis and Treatment Strategy: A Literature Review. Cells. 2019 Aug 2;8(8):818. doi: 10.3390/cells8080818.
4. Udagawa N., Takahashi N., Akatsu T., Tanaka H., Sasaki T., Nishihara T., Koga T., Martin T.J., Suda T. Origin of osteoclasts: Mature monocytes and macrophages are capable of differentiating into osteoclasts under a suitable microenvironment prepared by bone marrow-derived stromal cells. Proc Natl. Acad. Sci. USA. 1990;87:7260–7264. doi: 10.1073/pnas.87.18.7260.
5. Sun Y, Li J, Xie X, Gu F, Sui Z, Zhang K, Yu T. Recent Advances in Osteoclast Biological Behavior. Front Cell Dev Biol. 2021 Dec 8;9:788680. doi: 10.3389/fcell.2021.788680.
6. Trang NM, Kim EN, Lee HS, Jeong GS. Effect on Osteoclast Differentiation and ER Stress Downregulation by Amygdalin and RANKL Binding Interaction. Biomolecules. 2022 Feb 4;12(2):256. doi: 10.3390/biom12020256.
7. Tenshin H, Teramachi J, Ashtar M, Hiasa M, Inoue Y, Oda A, et al.. TGF-β-activated kinase-1 inhibitor LL-Z1640-2 reduces joint inflammation and bone destruction in mouse models of rheumatoid arthritis by inhibiting NLRP3 inflammasome, TACE, TNF-α and RANKL expression. Clin Transl Immunology. 2022 Jan 19;11(1):e1371. doi: 10.1002/cti2.1371.

8. Tanaka S. RANKL is a therapeutic target of bone destruction in rheumatoid arthritis. F1000Res. 2019 Apr 23;8:F1000 Faculty Rev-533. doi: 10.12688/f1000research.17296.1.
9. Sun Y, Li J, Xie X, Gu F, Sui Z, Zhang K, Yu T. Recent Advances in Osteoclast Biological Behavior. Front Cell Dev Biol. 2021 Dec 8;9:788680. doi: 10.3389/fcell.2021.788680.
10. Moorer MC, Riddle RC. Regulation of Osteoblast Metabolism by Wnt Signaling. Endocrinol Metab (Seoul). 2018 Sep;33(3):318–330. doi: 10.3803/EnM.2018.33.3.318. Epub 2018 Aug 14.
11. Lojk J, Marc J. Roles of Non-Canonical Wnt Signalling Pathways in Bone Biology. Int J Mol Sci. 2021 Oct 7;22(19):10840. doi: 10.3390/ijms221910840.
12. Jiang H, Zhang Z, Yu Y, Chu HY, Yu S, Yao S, et al. Drug Discovery of DKK1 Inhibitors. Front Pharmacol. 2022 Mar 9;13:847387. doi: 10.3389/fphar.2022.847387.
13. Parra-Torres AY, Enríquez J, Jiménez-Ortega RF, Patiño N, Castillejos-López MJ, Torres-Espíndola LM, et al. Expression profiles of the Wnt/β-catenin signaling-related extracellular antagonists during proliferation and differentiation in human osteoblast-like cells. Exp Ther Med. 2020 Dec;20(6):254. doi: 10.3892/etm.2020.9384. Epub 2020 Oct 23.
14. Zhang L, Tang Y, Zhu X, Tu T, Sui L, Han Q, et al. Overexpression of MiR-335-5p Promotes Bone Formation and Regeneration in Mice. J Bone Miner Res. 2017 Dec;32(12):2466–2475. doi: 10.1002/jbmr.3230. Epub 2017 Aug 28.
15. Zhang J, Tu Q, Bonewald LF, He X, Stein G, Lian J, et al. Effects of miR-335-5p in modulating osteogenic differentiation by specifically downregulating Wnt antagonist DKK1. J Bone Miner Res. 2011 Aug;26(8):1953–63. doi: 10.1002/jbmr.377.
16. Bellavia D, De Luca A, Carina V, Costa V, Raimondi L, Salamanna F, et al. Deregulated miRNAs in bone health: Epigenetic roles in osteoporosis. Bone. 2019 May;122:52–75. doi: 10.1016/j.bone.2019.02.013. Epub 2019 Feb 14.
17. Sun Y, Li J, Xie X, Gu F, Sui Z, Zhang K, Yu T. Recent Advances in Osteoclast Biological Behavior. Front Cell Dev Biol. 2021 Dec 8;9:788680. doi: 10.3389/fcell.2021.788680.
18. Soós B, Szentpétery Á, Raterman HG, Lems WF, Bhattoa HP, Szekanecz Z. Effects of targeted therapies on bone in rheumatic and musculoskeletal diseases. Nat Rev Rheumatol. 2022 May;18(5):249–257. doi: 10.1038/s41584-022-00764-w. Epub 2022 Mar 10. [19] Shaw AT, Yan J, Kuhstoss SA, Charles JF, Gravallese EM. Dickkopf-1 directs periosteal bone formation in two murine models of inflammatory arthritis. Scand J Rheumatol. 2022 Mar 11:1–5. doi: 10.1080/03009742.2022.2040136. Epub ahead of print.
19. Luo C, Xu W, Tang X, Liu X, Cheng Y, Wu Y, et al. Canonical Wnt signaling works downstream of iron overload to prevent ferroptosis from damaging osteoblast differentiation. Free Radic Biol Med. 2022 Aug 1;188:337–350. doi: 10.1016/j.freeradbiomed.2022.06.236. Epub 2022 Jun 23.
20. Rai D, Tripathi AK, Sardar A, Pandey AR, Sinha S, Chutani K, et al.. A novel BMP2 secretagogue ameliorates glucocorticoid induced oxidative stress in osteoblasts by activating NRF2 dependent survival while promoting Wnt/β-catenin mediated osteogenesis. Free Radic Biol Med. 2022 Aug 10:S0891-

5849(22)00514-7
. doi: 10.1016/j.freeradbiomed.2022.08.007. Epub ahead of print.

21. Amarasekara DS, Yun H, Kim S, Lee N, Kim H, Rho J. Regulation of Osteoclast Differentiation by Cytokine Networks. Immune Netw. 2018 Feb 7;18(1):e8. doi: 10.4110/in.2018.18.e8.
22. Udagawa N, Koide M, Nakamura M, Nakamichi Y, Yamashita T, Uehara S, Kobayashi Y, et al.. Osteoclast differentiation by RANKL and OPG signaling pathways. J Bone Miner Metab. 2021 Jan;39(1):19–26. doi: 10.1007/s00774-020-01162-6. Epub 2020 Oct 20.
23. Liu LN, Mao YM, Zhao CN, Wang H, Yuan FF, Li XM, et al. Circulating Levels of Osteoprotegerin, Osteocalcin and Osteopontin in Patients with Rheumatoid Arthritis: A Systematic Review and Meta-Analysis. Immunol Invest. 2019 Feb;48(2):107–120. doi: 10.1080/08820139.2018.1510957. Epub 2018 Sep 6.
24. Li N, Jiang L, Cai Y, Liu JY, Zhao T, Kong N, Yu Y, Xuan DD, Zou H, Xue Y, Wan W. The correlation between interleukin-34 and bone erosion under ultrasound in rheumatoid arthritis. Mod Rheumatol. 2020 Mar;30(2):269–275. doi: 10.1080/14397595.2019.1593576. Epub 2019 Apr 16.
25. Ling Y, Yang J, Hua D, Wang D, Zhao C, Weng L, et al.. ZhiJingSan Inhibits Osteoclastogenesis via Regulating RANKL/NF-κB Signaling Pathway and Ameliorates Bone Erosion in Collagen-Induced Mouse Arthritis. Front Pharmacol. 2021 May 28;12:693777. doi: 10.3389/fphar.2021.693777.
26. Jura-Półtorak A, Szeremeta A, Olczyk K, Zoń-Giebel A, Komosińska-Vassev K. Bone Metabolism and RANKL/OPG Ratio in Rheumatoid Arthritis Women Treated with TNF-α Inhibitors. J Clin Med. 2021 Jun 29;10(13):2905. doi: 10.3390/jcm10132905.
27. Gong M, Ma J, Guillemette R, Zhou M, Yang Y, Yang Y, Hock JM, Yu X. miR-335 inhibits small cell lung cancer bone metastases via IGF-IR and RANKL pathways. Mol Cancer Res. 2014 Jan;12(1):101–10. doi: 10.1158/1541-7786.MCR-13-0136. Epub 2013 Aug 21. PMID: 23966614.
28. Feldmann M, Brennan FM, Maini RN. Role of cytokines in rheumatoid arthritis. Annu Rev Immunol. 1996;14:397–440. doi: 10.1146/annurev.immunol.14.1.397.

Tables

Table 1 Grouping of experimental animals and method of administration of the model

Group	N	Medication
Blank	12	Normal saline
CIA	12	Normal saline
Kidney deficiency pattern	12	Normal saline
Kidney deficiency pattern CIA	12	Normal saline
CIA+ WBT	12	WBT 0.63g/kg QD
Kidney deficiency pattern CIA +WBT	12	WBT 0.63g/kg QD
Kidney deficiency pattern CIA +WBT	12	WBT 0.63g/kg QD
CIA+ MTX	12	MTX 1.05mg/kg QW; Normal saline

Table 2 Primers for the experiment

Target Name	Primer	
β-Actin	β-Actin-F	CTGAACGTGAAATTGTCCGAGA
	β-Actin-R	TTGCCAATGGTGATGACCTG
miR-335-5p	miR-335-5p(R)-F	GTCGTATCCAGTGCAGGGTCCG
	miR-335-5p(R)-R	AGGTATCGCACTGGATACGACA
OPG(R)	OPG(R)-F	ACATCATTGAATGGACAACCCAG
	OPG(R)-R	TGCCAGGAGCACATTTGTCA
RANKL(R)	RANKL(R)-F	CACACGAGGGTCCGCTGCATC
	RANKL(R)-R	TGCAGACCACCTGACCCAGTCC

Table 3 Concentrations of RANKL and OPG and RANKL/OPG ratio in rat serum

Group	RANKL (ng/l)	OPG (pmol/l)	RANKL/OPG (ng/pmol)
A	113.2±36.75	52.48±2.395	2.161±0.7180
B	196.3±10.68*	26.85±13.51**	8.866±4.401
C	144.1±45.16	30.19±2.372**	4.878±1.931

Note: A. Blank control group, B. Kidney deficiency pattern CIA group, C. Kidney deficiency pattern CIA+WBT group; compared with blthe ank control group, *P<0.05, **P<0.01

Table 4 Serum IL-1β and IL-4 concentrations of rats in each group

Group	IL-1β(ng/L)	IL-4(pg/ml)
A	41.42±1.98	19.49±5.18
B	41.82±1.80	19.41±0.95
C	69.51±0.895**	9.39±0.95**
D	50.92±1.35	13.15±1.93
E	58.76±3.48	19.49±5.19
F	74.75±0.94**	7.141±0.66**
G	56.91±8.15##	9.86±0.39#

Note: A. Blank control group; B. Kidney deficiency pattern group; C. CIA group; D. CIA+WBT group; E. CIA+MTX group; F. Kidney deficiency pattern CIA group; G. Kidney deficiency pattern CIA+WBT group; compared with blank control group, **P<0.01, compared with kidney deficiency pattern CIA group, # P< 0.05 ## P<0.01, compared with CIA group P<0.01

Figures

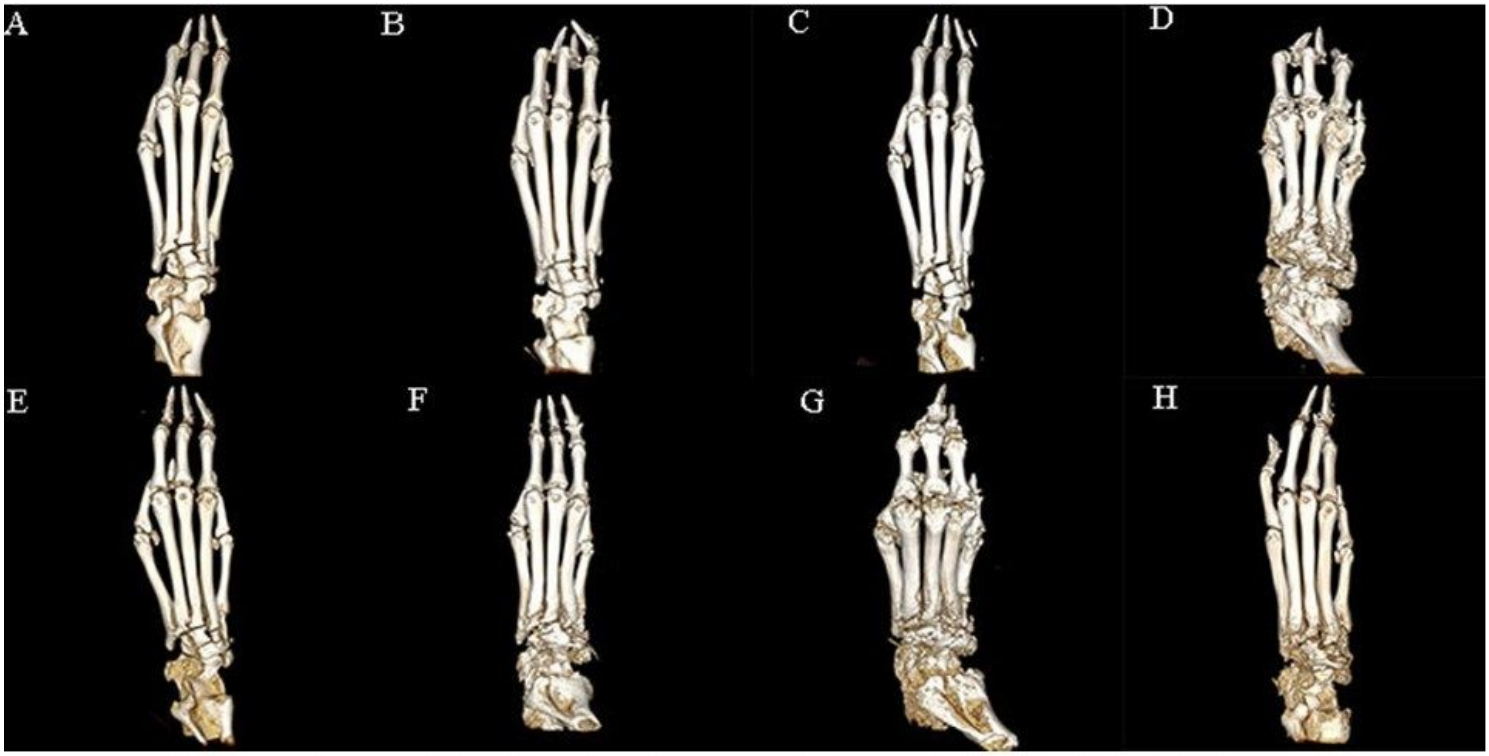

Figure 1 Each group's micro-CT of three dimensions images. **A**. Blank control group; **B.** Kidney deficiency pattern group; **C.** Kidney deficiency pattern+WBT group; **D.** CIA group; **E.** CIA+WBT group; **F.** CIA+MTX group; **G.** Kidney deficiency pattern CIA group; **H.** Kidney deficiency pattern CIA+WBT group.

Figure 1

See image above for figure legend.

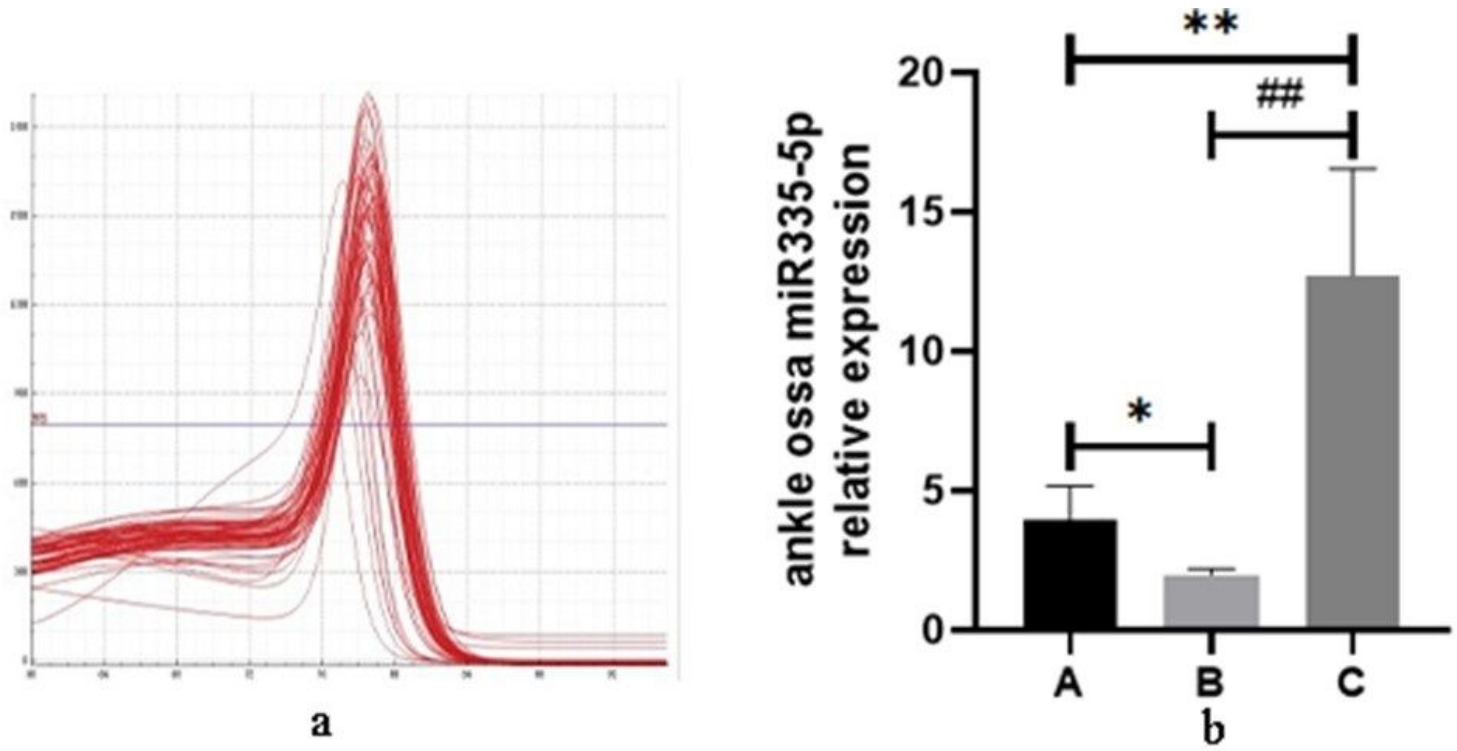

Figure 2 Expression of miR335-5p mRNA in ankle bone tissue of rats in each group. **A.** Blank control group; **B.** Kidney deficiency pattern CIA group; **C.** Kidney deficiency pattern CIA+WBT group; compared with blank control group, *P<0.05, **P<0.01; compared with kidney deficiency pattern CIA group, ##P<0.01; a miR335-5p lysis curve, b miR335-5p relative expression

Figure 2

See image above for figure legend.

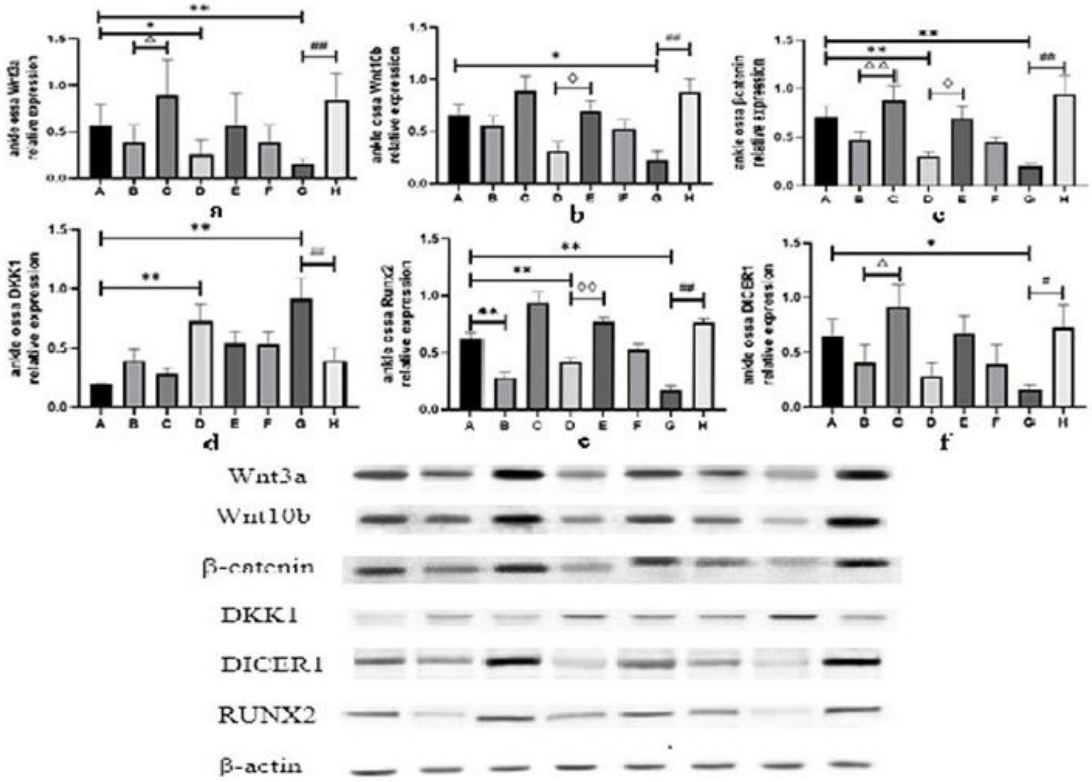

Figure 3 Relative expressions of Wnt3a, Wnt10b, β-catenin, DKK1, RUNX2 and DICER1 in the bone tissue of the ankle joint of rats in each group. Note: **A**. Blank control group; **B.** Kidney deficiency pattern group; **C.** Kidney deficiency pattern+WBT group; **D.** CIA group; **E.** CIA+WBT group; **F.** CIA+MTX group; **G.** Kidney deficiency pattern CIA group; **H.** Kidney deficiency pattern CIA+WBT group. The results were compared with the blank control group, *P<0.05, **P<0.01, # P< 0.05 ## P<0.01, △ P< 0.05 △ P<0.01, △ P<0.01, ◇ P< 0.05 ◇◇P<0.01, compared with the CIA group; a: Wnt3a, b:Wnt10b, c: β-catenin, d:DKK1, e: RUNX2, f: DICER1

Figure 3

See image above for figure legend.

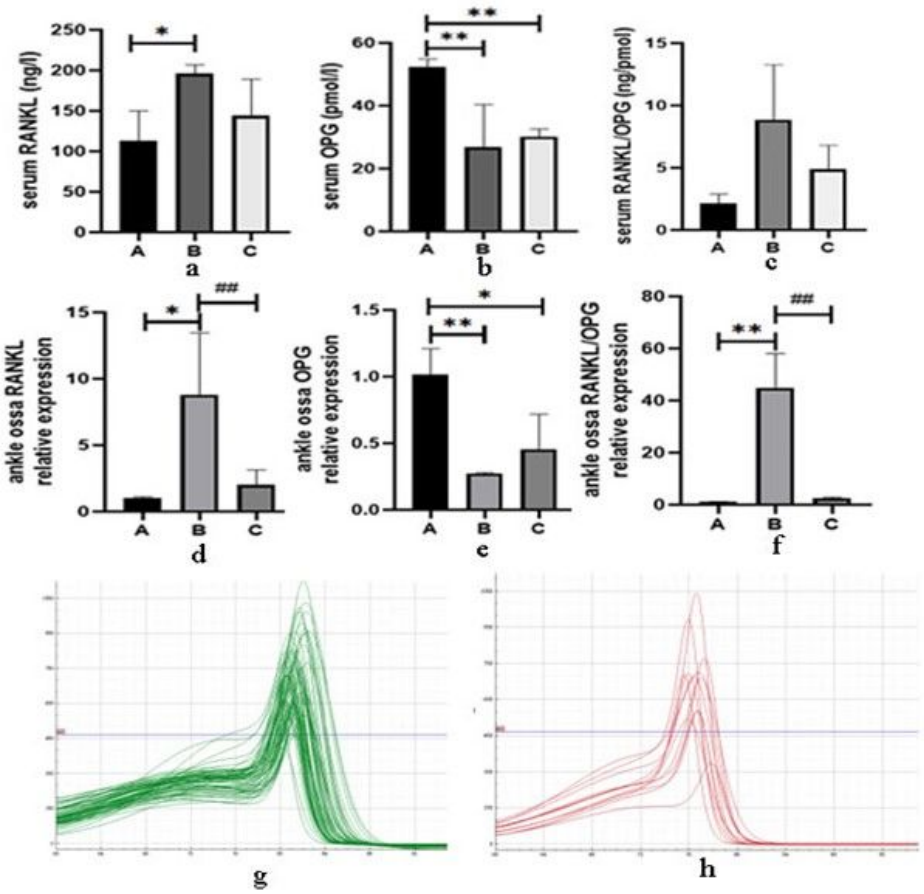

Figure 4 Expression of RANKL and OPG in serum and ankle bone tissue of rats in each group. **A**. Blank control group, **B.** Kidney deficiency pattern CIA group, **C.** Kidney deficiency pattern CIA+WBT group; compared with the blank control group, *P<0.05, **P<0.01; compared with kidney deficiency pattern CIA group, ##P<0.01; **a** serum RANKL, **b** serum OPG, **c** serum RANKL/OPG, **d** bone tissue RANKL, **e** bone tissue OPG, f Bone tissue RANKL/OPG, **g** RANKL melting curve **h** OPG lysis curve

Figure 4

See image above for figure legend.

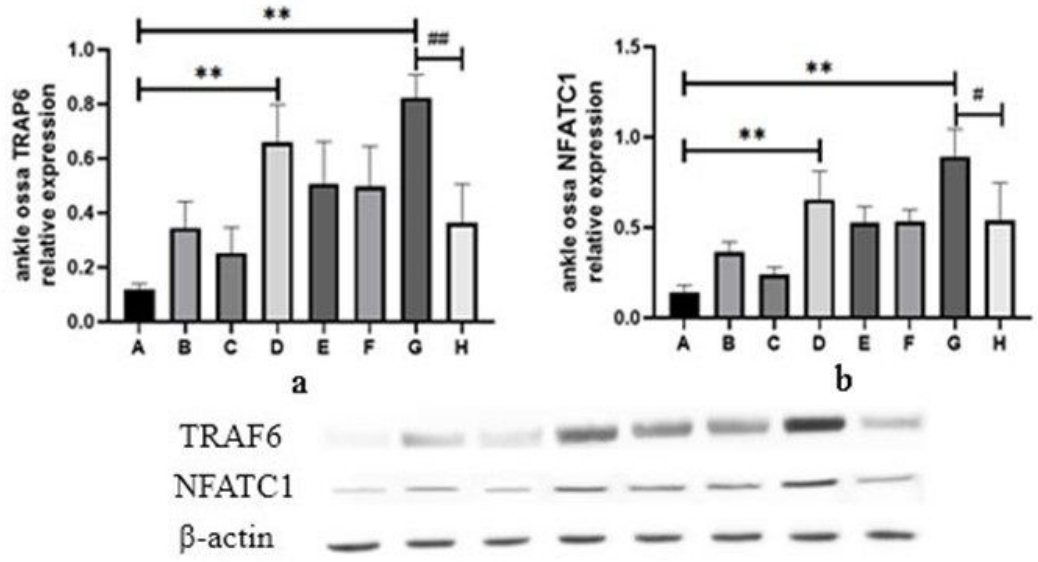

Figure 5 Values of TRAP6 and NFATC1 in ankle bone tissue of rats in each group. **A.** Blank control group; **B.** Kidney deficiency pattern group; **C.** Kidney deficiency pattern +WBT group; **D.** CIA group; **E.** CIA+WBT group; **F.** CIA+MTX group; **G.** Kidney deficiency pattern CIA group; H. Kidney deficiency pattern CIA+WBT group; compared with blank control group, **P<0.01; compared with kidney deficiency pattern CIA group, # P< 0.05 ## P<0.01; **a** TRAP6, **b** NFATC1

Figure 5

See image above for figure legend.

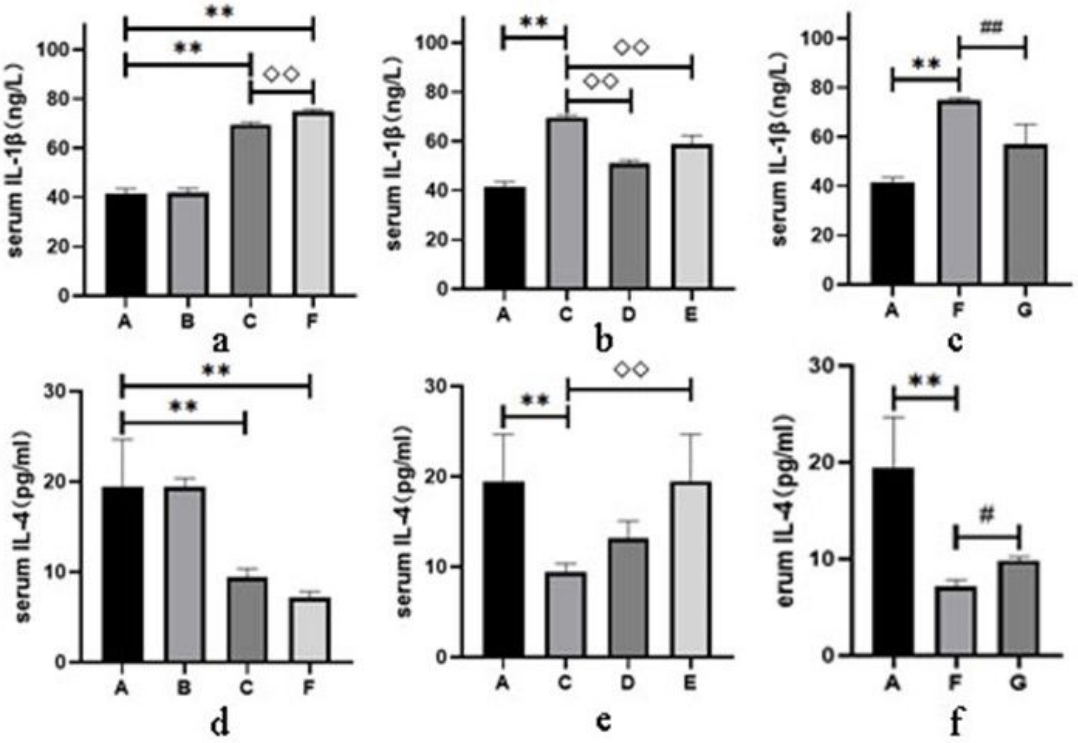

Figure 6 Effect of WBT on serum IL-1β and IL-4 in each group of rats. **A.** Blank control group; **B.** Kidney deficiency pattern group; **C.** CIA group; **D.** CIA+WBT group; **E.** CIA+MTX group; **F.** Kidney deficiency pattern CIA group; **G.** Kidney deficiency pattern CIA+WBT group; compared with blank control group, **P<0.01, compared with kidney deficiency pattern CIA group, ## P< 0.05 ## P<0.01, compared with CIA group ◇◇P<0.01 ; a-c IL-1β, d-f IL-4

Figure 6

See image above for figure legend.

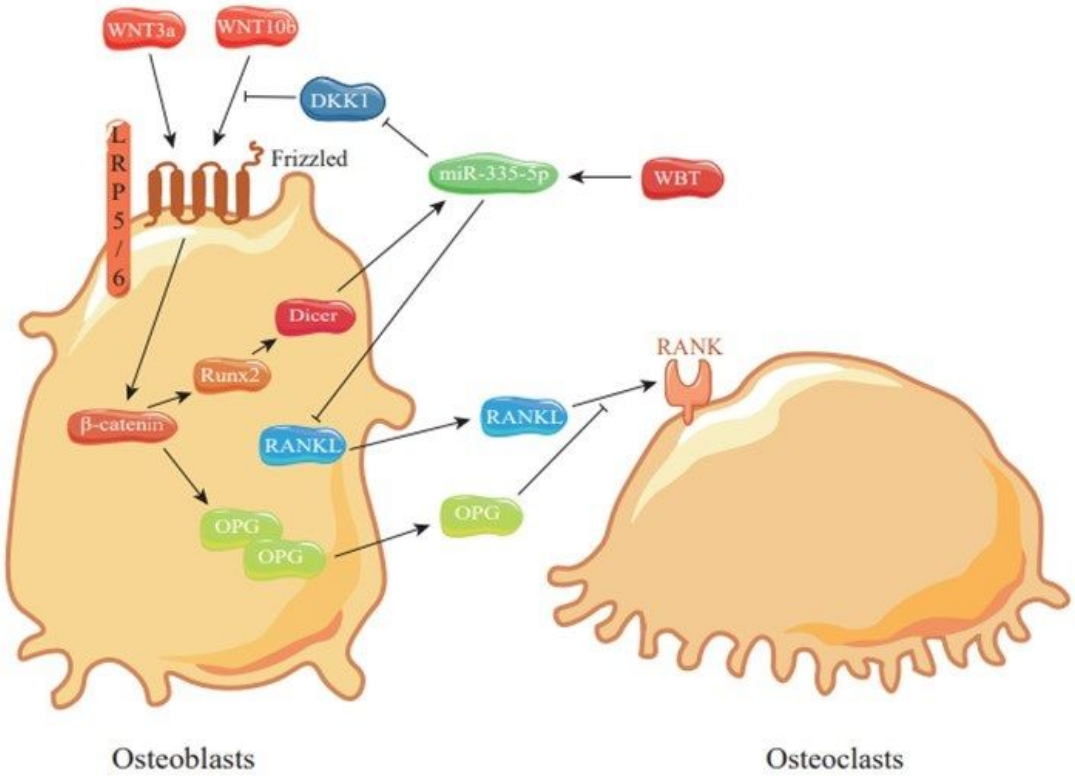

Figure 7 WBT regulates osteogenic balance through miR335-5p in the treatment of bone destruction in RA

Figure 7

See image above for figure legend.